Silver compounds in synthetic chemistry. Part 3. 4-Tetrafluoropyridyl silver(I), AgC_5F_4N – A reagent for redox transmetallations with group 12–14 elements ☆

Wieland Tyrra *, Said Aboulkacem, Ingo Pantenburg

Institut für Anorganische Chemie, Universität zu Köln, Greinstrasse 6, D-50939 Köln, Germany

Abstract

4-Tetrafluoropyridyl silver(I), AgC_5F_4N, has been obtained from $Me_3SiC_5F_4N$ and AgF in nearly quantitative yield. Reactions with bis(triphenylphosphoranyliden)ammonium chloride, [PNP]Cl, gave crystalline material of the composition $[PNP][Ag(C_5F_4N)_2]$. Redox transmetallations of AgC_5F_4N and group 12–14 elements Zn, Cd, Hg, Ga, In, Sn yielded the corresponding 4-tetrafluoropyridyl element compounds. The molecular structures of $[PNP][Ag(C_5F_4N)_2]$, $Hg(C_5F_4N)_2$, $Ga(C_5F_4N)_3 \cdot EtCN \cdot H_2O$, $In(C_5F_4N)_3 \cdot 2EtCN$ and $Sn(C_5F_4N)_4$ are discussed.
© 2005 Elsevier B.V. All rights reserved.

Keywords: 4-Tetrafluoropyridyl; Silver; Synthesis; Crystal structure

1. Introduction

The tetrafluoropyridyl group has already attracted considerable interest in transition metal [1,2] as well as main group metal chemistry [3]. On the basis of theoretical calculations [4], the electron-withdrawing effect of the C_5F_4N ligand should be considered to be higher than that of the isolobal C_6F_5 group. Together with the knowledge that perfluoroorgano silver(I) compounds with strong electron-withdrawing organic ligands can be synthesized conveniently and are versatile tools for redox transmetallations [5–8], we studied the reactions of AgC_5F_4N and elements of groups 12–14.

2. Results and discussion

2.1. Syntheses of 4-tetrafluoropyridyl silver(I), AgC_5F_4N and bis(triphenylphosphoranyliden)ammonium bis (4-tetrafluoropyridyl)argentate, $[PNP][Ag(C_5F_4N)_2]$

4-Tetrafluoropyridyl silver(I), AgC_5F_4N, is conveniently accessible via the reactions of the corresponding silane, $Me_3SiC_5F_4N$, and silver(I) fluoride as already outlined for other perfluorinated groups [5–8]. In propionitrile solution – other solvents are also suitable [6] – the reaction proceeds selectively to give AgC_5F_4N in nearly quantitative yield (Eq. (1)).
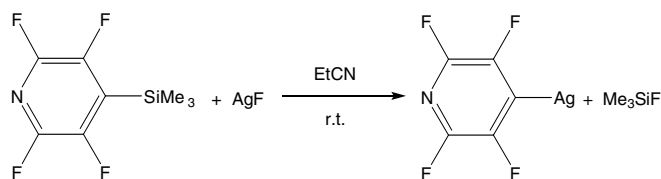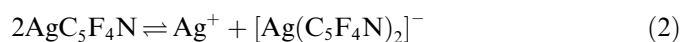

$$\tag{1}$$

Exchange processes in solution between a "neutral" and an "ionic" species appear to be too fast for the NMR time

scale, i.e., only two well-resolved signal groups are observed in the ^{19}F NMR spectra irrespective of the solvent (Eq. (2)). These experiences are in contrast to results known for perfluoroalkyl silver(I) derivatives [9].

$$2AgC_5F_4N \rightleftharpoons Ag^+ + [Ag(C_5F_4N)_2]^- \qquad (2)$$

Unfortunately, single crystals of AgC_5F_4N could not be obtained. As previously outlined for two related examples [7,10], the reaction of AgC_5F_4N and bis(triphenylphosphoranyliden)ammonium chloride, [PNP]Cl, in a stoichiometric ratio of 2:1 gave crystalline $[PNP][Ag(C_5F_4N)_2]$ suitable for XRD measurements (Eq. (3)).

$$(3)$$
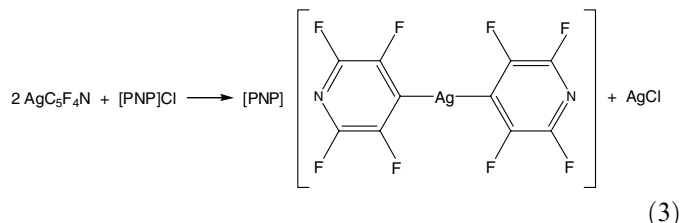
Results of mass spectrometric investigations (negative ESI) gave evidence of the complex equilibria in solution. For redox transmetallations, AgC_5F_4N was prepared according to Eq. (1) and used without further purification.

## 2.2. Molecular structure of [PNP][Ag(C₅F₄N)₂]

$[PNP][Ag(C_5F_4N)_2]$ (1) crystallizes in the monoclinic space group $P2_1/c$ (no. 14) with 4 molecules per unit cell (Table 1; Fig. 1). The lattice is built up by well-separated ion pairs of the [PNP] cations and the argentate anions. The anions are layered in cavities formed by the framework of the bulky [PNP] cations without significant F–H contacts (>241 pm). The silver atom is quasi-linear co-ordinated as found for all perfluoroorganosilver(I) derivatives crystallographically characterized so far. This is obvious in the structures of homoleptic [8,10–12] as well as heteroleptic derivatives [7,11,13]. The planar rings are tilted at $83.5 \pm 0.5°$ with respect to each other.

The C–Ag–C bond angle of 173.0(1)° only slightly deviates from linearity; Ag–C bond lengths are found to be 210.8(4) and 211.2(4) pm. These values are in good agreement with reported data [7,8,10–12] implying similar electronic distributions around the silver atoms irrespective of the perfluoroorgano group.

2.3. Redox transmetallations of AgC₅F₄N and elements of groups 12–14

AgC_5F_4N shows excellent oxidizing abilities in reactions with elemental zinc, cadmium, mercury (Eq. (4)), gallium, indium (Eq. (5)), and tin (Eq. (6)). All reactions proceed more or less indiscriminately to give the corresponding 4-tetrafluoropyridyl element compounds and elemental silver beside traces of tetrafluoropyridine.

$$2AgC_5F_4N + M \rightarrow M(C_5F_4N)_2 \cdot nEtCN + 2Ag$$
$$M = Zn, Cd \ (n = 2), Hg \ (n = 0) \qquad (4)$$
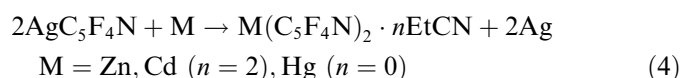
$Zn(C_5F_4N)_2$ and $Cd(C_5F_4N)_2$ were isolated as waxy solids presumably as 1:2 adducts [14] with EtCN. Both compounds are extremely sensitive to moisture. They react spontaneously with water under formation of tetrafluoropyridine. By contrast, $Hg(C_5F_4N)_2$ is not affected by moisture. It has been obtained free of co-ordinating solvent molecules as crystalline material (cf. Section 2.4).

In a similar manner reactions proceed with the group 13 elements gallium and indium. Due to the passivation of aluminium, no reaction was observed with aluminium shots, while with elemental thallium the oxidation is finished on the oxidation step of thallium(I), because the oxidation potential of AgC_5F_4N is too low [8]. As a consequence, compounds of general formula $[Tl^I \cdot nEtCN][Ag(C_5F_4N)_2]$ were formed.

$$3AgC_5F_4N + M \rightarrow M(C_5F_4N)_3 \cdot nEtCN + 3Ag$$
$$M = Ga \ (n = 1), In \ (n = 2) \qquad (5)$$
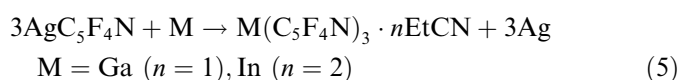
Results of the single crystal structure analyses of $Ga(C_5F_4N)_3 \cdot EtCN \cdot H_2O$ and $In(C_5F_4N)_3 \cdot 2EtCN$ are presented in Sections 2.5 and 2.6, respectively.

Elemental tin is oxidized by AgC_5F_4N in a primary step to a compound presumed to be "$Ag[Sn^{II}(C_5F_4N)_3]$" [15]. This intermediate is converted into $Sn^{IV}(C_5F_4N)_4$ and elemental silver in a sublimation apparatus after extended heating to 230 °C at 0.1 mbar.

$$4AgC_5F_4N + Sn \rightarrow Sn(C_5F_4N)_4 + 4Ag \qquad (6)$$

Unfortunately, low solubility of $Sn(C_5F_4N)_4$ in common organic solvents prevented from a complete characterization in solution. The results of XRD measurement are summarized in Section 2.7.

Reactions with elemental germanium remained unsuccessful. Rising the temperature up to 60 °C for 48 h did not give even spectroscopic evidence for the formation of GeC_5F_4N derivatives. Reactions with elemental lead proceeded in a similar manner as with thallium to give "$Pb^{II}[Ag(C_5F_4N)_2]_2$"; however, thermal decomposition of the raw material did not yield $Pb(C_5F_4N)_4$, as expected [8], but 4,4′-octafluorobipyridyl.

2.4. Molecular structure of Hg(C₅F₄N)₂

$Hg(C_5F_4N)_2$ (2) crystallizes in the monoclinic space group $P2_1/c$ (no. 14) with 8 molecules per unit cell. The molecular structure of $Hg(C_5F_4N)_2$ is depicted in Fig. 2, the packing scheme in Fig. 3. The compound crystallizes in parallel infinite zig-zag chains of two crystallographically independent $Hg(C_5F_4N)_2$ molecules. Each mercury atom shows one significant Hg–N contact (284.8(7) and 287.0(8) pm) to one of the ring nitrogen atoms of adjacent $Hg(C_5F_4N)_2$ moieties within the chain. As a consequence, mercury atoms are T-shaped co-ordinated with N–Hg–C angles of 89.1(3)–98.3(3)°. This co-ordination appears to be a characteristic structural motif of many perfluoroorgano mercury compounds in the solid state [16].

Table 1
Crystal data and structure refinement parameters for [PNP][Ag(C$_5$F$_4$N)$_2$] (**1**), Hg(C$_5$F$_4$N)$_2$ (**2**), Ga(C$_5$F$_4$N)$_3$ · EtCN · H$_2$O (**3**), In(C$_5$F$_4$N)$_3$ · 2EtCN (**4**), and Sn(C$_5$F$_4$N)$_4$ (**5**)

Complex	**1**	**2**	**3**	**4**	**5**
Empirical formula	C$_{46}$H$_{30}$N$_3$F$_8$P$_2$Ag	C$_{10}$N$_2$F$_8$Hg	C$_{18}$H$_7$N$_4$F$_{12}$OGa	C$_{21}$H$_{10}$N$_5$F$_{12}$In	C$_{20}$N$_4$F$_{16}$Sn
Formula mass (g/mol)	946.54	500.71	593.00	675.16	718.93
Data collection					
Diffractometer			STOE IPDS II		
Radiation			Mo Kα (graphite monochromator, $\lambda = 71.073$ pm)		
T (K)	170(2)	170(2)	150(2)	150(2)	293(2)
Index range	$-12 \leqslant h \leqslant 12$,	$-12 \leqslant h \leqslant 12$,	$-16 \leqslant h \leqslant 15$,	$-12 \leqslant h \leqslant 12$,	$-15 \leqslant h \leqslant 15$,
	$-24 \leqslant k \leqslant 23$,	$-6 \leqslant k \leqslant 7$,	$-11 \leqslant k \leqslant 11$,	$-11 \leqslant k \leqslant 11$,	$-15 \leqslant k \leqslant 14$,
	$-30 \leqslant l \leqslant 30$	$-41 \leqslant l \leqslant 41$	$-26 \leqslant l \leqslant 25$	$-35 \leqslant l \leqslant 33$	$-9 \leqslant l \leqslant 9$
Rotation angle range	$0° \leqslant \omega \leqslant 180°$;	$0° \leqslant \omega \leqslant 180°$;	$0° \leqslant \omega \leqslant 180°$;	$0° \leqslant \omega \leqslant 180°$;	$0° \leqslant \omega \leqslant 180°$;
	$\psi = 0°$	$\psi = 0°$	$\psi = 0°$	$\psi = 0°$	$\psi = 0°$
	$0° \leqslant \omega \leqslant 14°$;	$0° \leqslant \omega \leqslant 86°$;	$0° \leqslant \omega \leqslant 158°$;	$0° \leqslant \omega \leqslant 94°$;	$0° \leqslant \omega \leqslant 126°$;
	$\psi = 90°$	$\psi = 90°$	$\psi = 90°$	$\psi = 0°$	$\psi = 90°$
Increment	$\Delta\omega = 2°$	$\Delta\omega = 2°$	$\Delta\omega = 2°$	$\Delta\omega = 1°$	$\Delta\omega = 2°$
Number of images	97	133	169	274	153
Exposure time (min)	12	7	4	7	4
Detector distance (mm)	120	140	120	120	120
2θ Range (°)	1.9–54.8	1.6–50.5	1.9–54.8	1.9–54.8	1.9–54.8
Total data collected	33 700	18 567	30 785	29 497	14 180
Unique data	9036	3945	4830	5494	1264
Observed data	5508	2827	3727	4362	965
R_{merg}	0.0579	0.0605	0.1456	0.0476	0.0367
Absorption correction			Numerical, after crystal shape optimization [44,45]		
Minimum/maximum transmission	0.8251/0.9336	0.1012/0.2583	none	0.7582/0.8963	0.7742/0.8749
Crystallographic data [43]					
Crystal size (mm)	$0.2 \times 0.2 \times 0.15$	$0.2 \times 0.2 \times 0.1$	$0.3 \times 0.3 \times 0.2$	$0.25 \times 0.25 \times 0.05$	$0.2 \times 0.05 \times 0.05$
Colour	Colourless	Colourless	Colourless	Colourless	Colourless
Habit	Polyhedron	Plate	Block	Plate	Column
Crystal system	Monoclinic	Monoclinic	Monoclinic	Monoclinic	Tetragonal
Space group	$P2_1/c$ (no. 14)	$P2_1/c$ (no. 14)	$P2_1/c$ (no. 14)	$P2_1/c$ (no. 14)	$P\bar{4}2_1c$ (no. 114)
a (pm)	983.0(1)	1079.5(1)	1245.6(7)	988.0(1)	1222.7(1)
b (pm)	1890.1(1)	593.1(1)	872.5(4)	902.9(1)	
c (pm)	2403.8(2)	3491.1(5)	2014.0(12)	2793.6(1)	751.6(1)
β (°)	114.24(1)	90.46(1)	92.47(5)	97.17(1)	
V (nm^3)	4.0724(7)	2.2370(5)	2.1870(2)	2.4725(1)	1.1235(2)
Z	4	8	4	4	2
ρ_{calc} (g cm^{-3})	1.544	2.973	1.801	1.814	2.125
μ (mm^{-1})	0.648	13.864	1.379	1.067	1.289
$F(0\,0\,0)$	1904	1808	1160	1312	2904
Structure analysis and refinement[a]					
Structure determination			SHELXS-97 [46] and SHELXL-93 [47]		
Number of variables	662	380	336	355	94
R indexes [$I > 2\sigma I$]	$R_1 = 0.0461$,	$R_1 = 0.0322$,	$R_1 = 0.0438$,	$R_1 = 0.0466$,	$R_1 = 0.0307$,
	$wR_2 = 0.1072$	$wR_2 = 0.0742$	$wR_2 = 0.1023$	$wR_2 = 0.1263$	$wR_2 = 0.0838$
R indexes (all data)	$R_1 = 0.0865$,	$R_1 = 0.0514$,	$R_1 = 0.0570$,	$R_1 = 0.0568$,	$R_1 = 0.0412$,
	$wR_2 = 0.1208$	$wR_2 = 0.0799$	$wR_2 = 0.1130$	$wR_2 = 0.1317$	$wR_2 = 0.0890$
Goodness of fit (S_{all})	0.938	0.890	1.051	1.045	1.073
Largest difference map in hole/peak (e 10^{-6} pm^{-3})	−1.034/1.755	−1.390/1.574	−0.415/0.572	−1.194/3.683	−0.415/0.532

$R_1 = \sum \|F_o| - |F_c\| / \sum |F_o|$, $wR_2 = [\sum w(|F_o|^2 - |F_c|^2)^2 / \sum w(|F_o|^2)^2]^{1/2}$, $S_2 = [\sum w(|F_o|^2 - |F_c|^2)^2/(n - p)]^{1/2}$, with $w = 1/[\sigma^2(F_o)^2 + (0.0669 \times P)^2]$ for **1**, $w = 1/[\sigma^2(F_o)^2 + (0.0523 \times P)^2]$ for **2**, $w = 1/[\sigma^2(F_o)^2 + (0.0464 \times P)^2 + (0.9379 \times P)]$ for **3**, $w = 1/[\sigma^2(F_o)^2 + (0.0939 \times P)^2]$ for **4** and $w = 1/[\sigma^2(F_o)^2 + (0.0579 \times P)^2 + (0.1387 \times P)]$ for **5**, where $P = (F_o^2 + 2F_c^2)/3$. $F_c^* = kF_c[1 + 0.001 \times |F_c|^2\lambda^3/\sin(2\theta)]^{-1/4}$.

[a] H atoms for **1** as well as the protons of the water molecule in **3** were taken from the difference Fourier map at the end of the refinement; protons of EtCN in **3** and **4** were placed in idealized positions and constrained to ride on their parent atom.
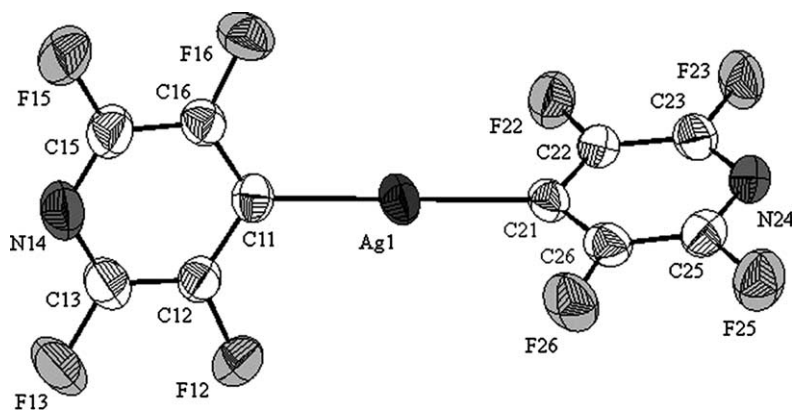
Fig. 1. Molecular structure of the anion in [PNP][Ag(C_5F_4N)$_2$] (**1**) showing the labeling scheme (thermal ellipsoids at the 50% probability level). Interatomic distances in pm and angles in degrees (with estimated standard deviations in parentheses): Ag1–C11 210.8(4), Ag1–C21 211.2(4), C11–Ag1–C21 173.0(1).
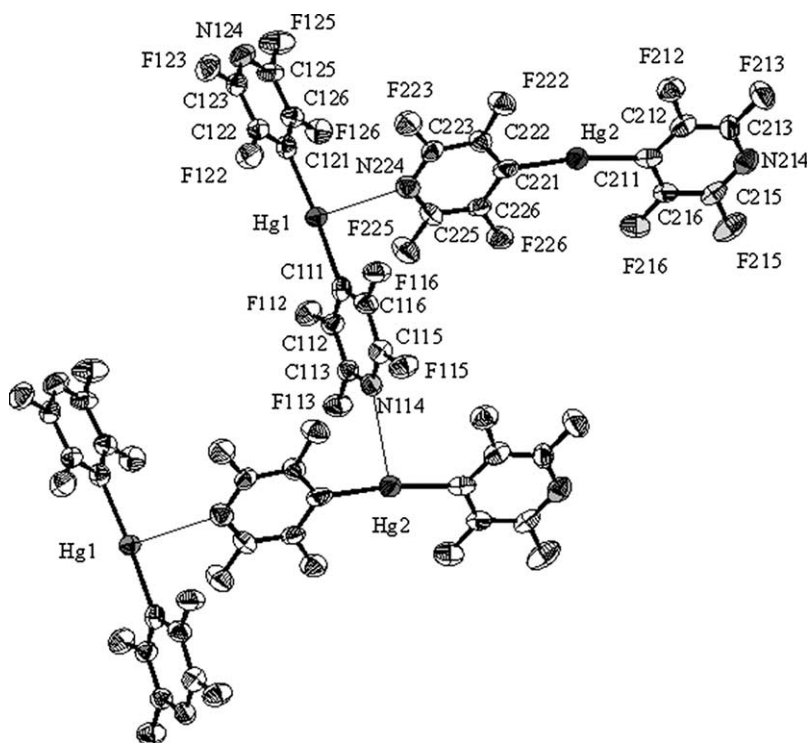

Fig. 2. View of Hg(C_5F_4N)$_2$ (**2**) showing the labeling scheme and the coordination environments of the mercury atoms (thermal ellipsoids at the 50% probability level). Interatomic distances in pm and angles in degrees (with estimated standard deviations in parentheses): Hg1–C111 209.3(9), Hg1–C121 209.9(9), Hg1–N224 287.0(8), Hg2–C211 207.3(11), Hg2–C221 206.1(10), Hg2–N114 284.8(7), C111–Hg1–C121 175.6(3), C211–Hg2–C221 172.1(3).

It must be noted that torsion or twist angles in both crystallographically independent Hg(C_5F_4N)$_2$ moieties deviate significantly from each other. The one has a value of $4.5 \pm 0.5°$, i.e., both aromatic rings may be regarded as co-planar, while a value of $60.0 \pm 0.5°$ is found for the other. In the case of approximately co-planar units, Hg–C bond lengths are shorter (206.1(10) and 207.3(11) pm) compared with those of twisted rings (209.3(9) and 209.9(9) pm). In both crystallographically independent units, C–Hg–C angles only slightly deviate from linearity (172.1(3)° and 175.6(3)°). These results fall in the good scope of structural data for homoleptic [17,18] as well as

heteroleptic [19] polyfluorinated phenyl mercury derivatives. Differences especially with respect to the twist angles and Hg–C bond length cannot be explained by differences in the electronic natures of the ligands and should therefore be attributed to packing considerations.

2.5. Molecular structure of Ga(C_5F_4N)$_3$ · EtCN · H_2O

Examples of structurally characterized gallium derivatives with strong electron withdrawing organic ligands are rare and limited to salts with the tetrakis(pentafluorophenyl)gallate anion, [Ga(C_6F_5)$_4$]⁻ [20–23], the
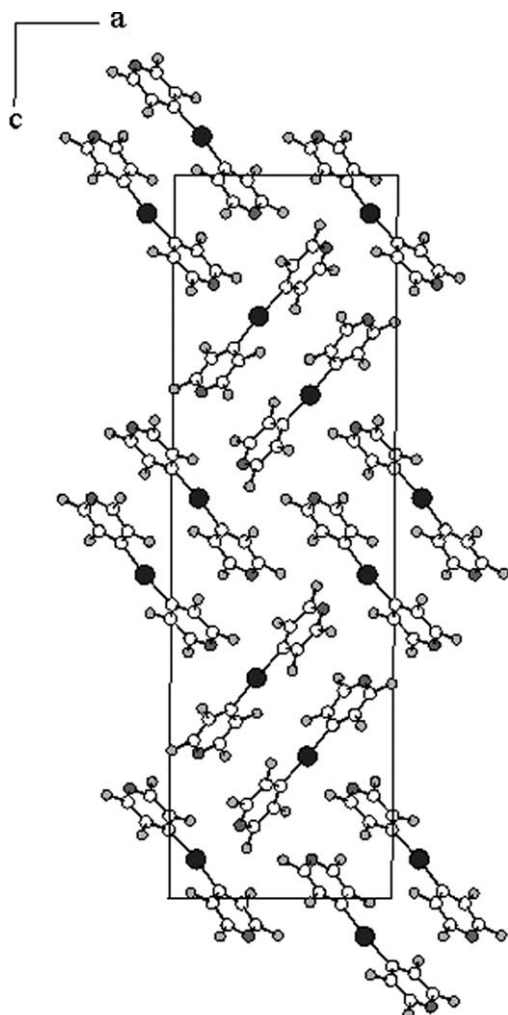
Fig. 3. The packing diagram for $Hg(C_5F_4N)_2$ (**2**) viewed along the crystallographic *b*-axis.

Fig. 4. View of $Ga(C_5F_4N)_3 \cdot EtCN \cdot H_2O$ (**3**) showing the labeling scheme and the coordination environment of the gallium atom (thermal ellipsoids at the 50% probability level). Interatomic distances in pm and angles in degrees (with estimated standard deviations in parentheses): Ga1–C11 199.5(3), Ga1–C21 199.4(3), Ga1–C31 199.9(3), Ga1–N41 227.0(3), Ga1–O51 221.9(2), C11–Ga1–C21 121.1(1), C11–Ga1–C31 116.4(1), C11–Ga1–N41 90.0(1), C11–Ga1–O51 91.9(1), C21–Ga1–C31 122.4(1), C21–Ga1–N41 88.4(1), C21–Ga1–O51 92.1(1), C31–Ga1–N41 89.6(1), C31–Ga1–O51 88.0(1), N41–Ga1–O51 177.4(1).

anions μ-fluorobis[tris(pentafluorophenyl)gallate], {[Ga-$(C_6F_5)_3]_2(\mu$-F)}$^-$ [24] and μ-hydroxybis[tris(pentafluorophenyl)gallate], {[Ga$(C_6F_5)_3]_2(\mu$-OH)}$^-$ [25] as well as the 1:1 complexes of $Ga(C_6F_5)_3$ with THF [26,27] and Et_2O [27].

All spectroscopic data of the product derived from the reaction of AgC_5F_4N with elemental gallium in EtCN prove that the primary formed compound $Ga(C_5F_4N)_3 \cdot EtCN$ is contaminated by a salt with the $[Ga(C_5F_4N)_4]^-$ anion. Single crystals were grown upon storing an *n*-pentane solution of the raw material at −21 °C over a period of two months.

$Ga(C_5F_4N)_3 \cdot EtCN \cdot H_2O$ (**3**) (Table 1, Fig. 4) crystallizes in the monoclinic space group $P2_1/c$ (no. 14) with 4 molecules per unit cell in a similar manner as In-$(C_5F_4N)_3 \cdot 2EtCN$ (Section 2.6). The tetrafluoropyridyl ligands reside in equatorial positions of a distorted trigonal bi-pyramid; Ga–C bond lengths do not deviate from those of covalent Ga–C (2c–2e) bonds [20–27]. Nitrogen and oxygen bonds of the linear, apical motif are elongated by approximately 10% compared with those in tetrahedral
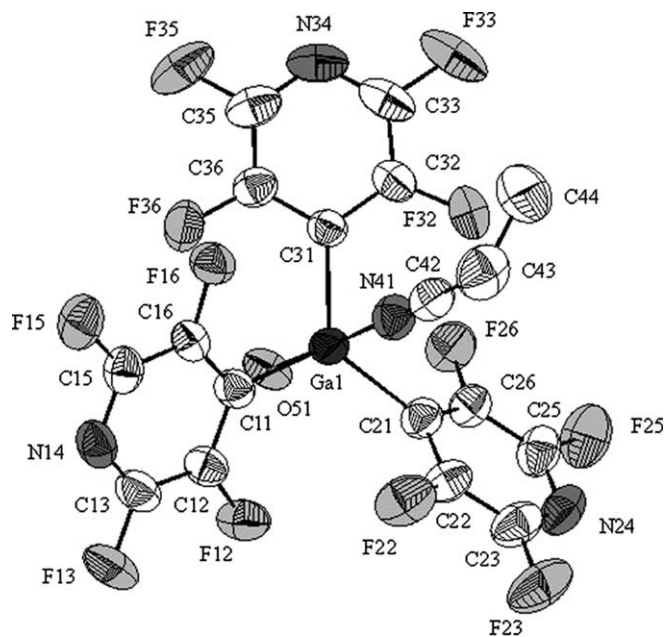
motifs (221.9(2) pm versus ca. 200 pm (Ga–O) [25–27]). There was found no evidence for intermolecular contacts. Neither the O–Ga–N angle (177.4(1)°) deviates significantly from linearity nor the sum of C–Ga–C angles (mean value 120.0° (116.4(1)°, 121.1(1)°, 122.4(1)°)) from planarity exhibiting real trigonal bi-pyramidal geometry for $Ga(C_5F_4N)_3 \cdot EtCN \cdot H_2O$. The unusual penta-coordination might be interpreted in terms of great electron deficiency at the gallium centre which is compensated by co-ordination of EtCN and one additional water molecule acting as donors.

2.6. Molecular structure of $In(C_5F_4N)_3 \cdot 2EtCN$

Examples of crystal structures of polyfluoroaryl indium compounds are to our knowledge rare and limited to three examples: $In(C_6F_5)Br_2 \cdot 2$ THF [28], $In(C_6F_5)_2(CH_2)_3$-NMe_2 [29], and $[PNP][In(C_6F_5)_4]$ [30].

$In(C_5F_4N)_3 \cdot 2EtCN$ (**4**) crystallizes in the monoclinic space group $P2_1/c$ (no. 14) with 4 molecules per unit cell (Table 1, Fig. 5). It exhibits well separated trigonal bipyramidal $In(C_5F_4N)_3 \cdot 2EtCN$ units without any significant intermolecular contacts. The aromatic rings occupy equatorial positions, while the propionitrile ligands reside in axial sites. In–C bond lengths vary from 216.5(4) to 217.6(3) pm and are in good agreement with known values for pentafluorophenyl compounds [28–30]. The mean value of the angles C–In–C of 119.7° only slightly deviates from
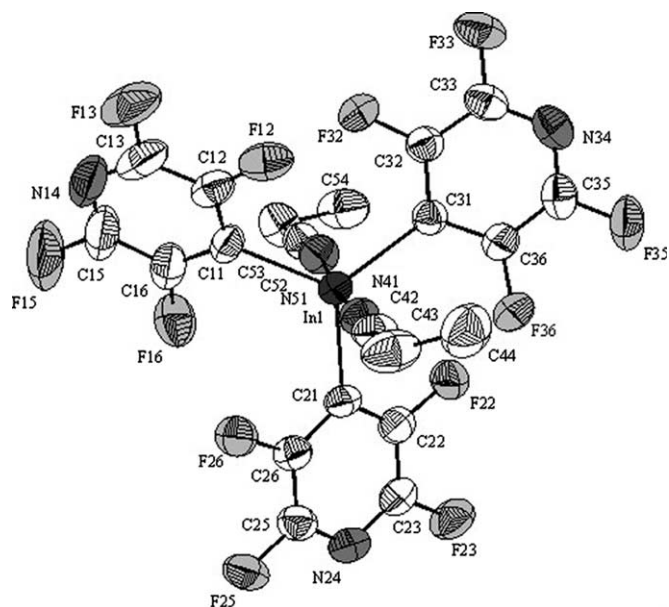
Fig. 5. Central projection of the asymmetric unit of In(C₅F₄N)₃ · 2EtCN (4) showing the atom numbering scheme (thermal ellipsoids at the 50% probability level). H atoms have been omitted for clarity. Interatomic distances in pm and angles in degrees (with estimated standard deviations in parentheses): In1–C11 217.2(4), In1–C21 217.6(3), In1–C31 216.5(4), In1–N41 238.1(4), In1–N51 244.6(4), C11–In1–C21 117.6(2), C21–In1–C31 121.2(1), C11–In1–C31 120.5(1), N41–In1–N51 176.0(1), C11–In1–N41 95.1(1), C11–In1–N51 87.4(1), C21–In1–N41 93.4(1), C21–In1–N51 88.2(1), C31–In1–N41 90.0(1), C31–In1–N51 86.1(1).

the ideal value of 120°. Approximate linearity is found for the N–In–N unit (176.0(1)°). As a consequence, the mean value of the C–In–N angles (90.0°) does not deviate from ideal relations although values vary from 86.1(1)° to 95.1(1)°. In–N contacts of 238.1(4) and 244.6(4) pm are longer than the sum of covalent radii (220 pm [31]) but significantly shorter than the sum of van der Waals radii (≈353 pm [32]). The surrounding on the indium atom matches well with that determined for In(S-2,4,6-(*i*-Pr₃)₃C₆H₂)₃ · 2MeCN [33].

2.7. Molecular structure of Sn(C₅F₄N)₄

Sn(C₅F₄N)₄ (5) crystallizes in the tetragonal space group ($P\bar{4}2_1c$, $Z = 2$) as tetraphenyltin [34] and tetrakis(3,5-dimethylphenyl)tin [35]. A view on the molecule is depicted in Fig. 6, while a view on the unit cell is given in Fig. 7. In the same manner as several related examples, such quasi-spherical molecules crystallize in tetragonal space groups allowing close packing.

Sn–C bonds of 215.5(4) pm (4×) are slightly elongated in comparison with Sn(C₆F₅)₄ (212.6(8) pm [36]) but in good agreement with those reported for Sn(C₆Cl₅)₄ [37] and fall absolutely into the range of bond lengths for SnAr₄ compounds structurally characterized so far (e.g. [34–38, and literature cited therein]). Differences in bond lengths appear to be independent of the electron withdrawing character of the aromatic system but might be attributed to packing

considerations. The first coordination sphere around the tin atom only slightly deviates from an ideal tetrahedron (111.0(1)° (4×), 106.5(2)° (2×)) and is in accordance with that of SnPh₄ [34] and Sn(C₆F₅)₄ [36].
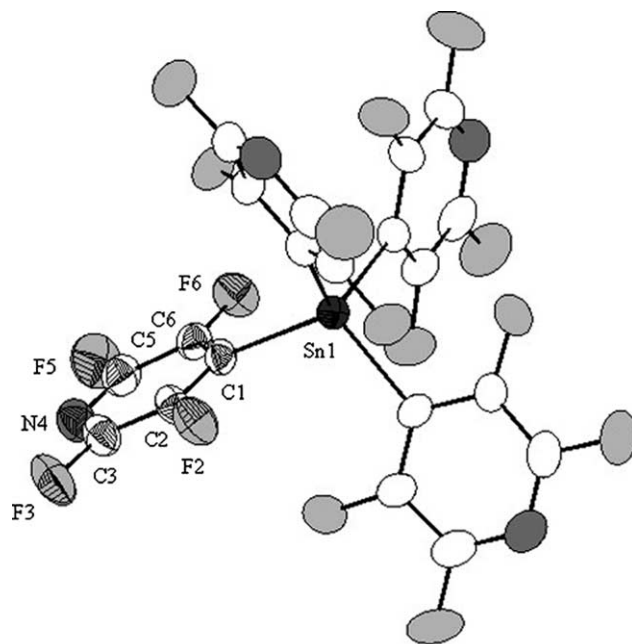
Fig. 6. View of Sn(C₅F₄N)₄ (5) showing the labeling scheme and the coordination environment of the tin atom (thermal ellipsoids at the 50% probability level). Symmetry-related atoms are drawn as empty ellipsoids. Interatomic distances in pm and angles in degrees (with estimated standard deviations in parentheses): Sn1–C1 215.5(4) (4×), C1–Sn1–C1 111.0(1) (4×), C1–Sn1–C1 106.5(2) (2×).
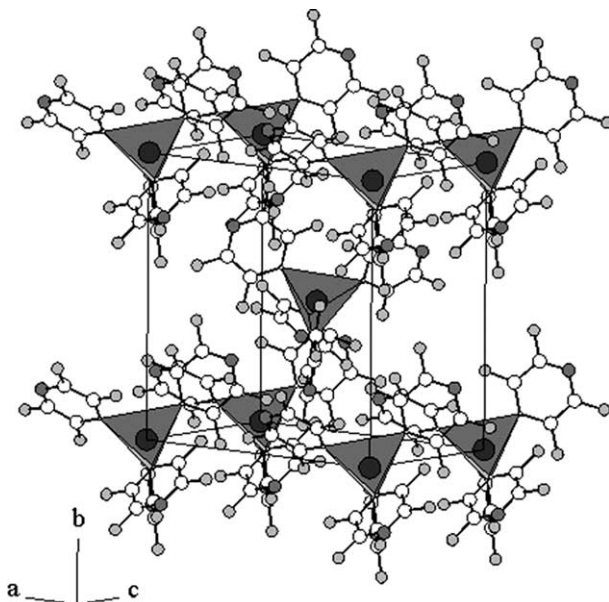
Fig. 7. The packing diagram for Sn(C₅F₄N)₄ (5).

3. Experimental

Schlenk techniques were used throughout most of the manipulations. NMR spectra were recorded on Bruker AC 200 (^{1}H, ^{19}F, ^{13}C) and AVANCE 400 ([199]Hg, [13]C{[19]F}) spectrometers. External standards were used in all cases (^{1}H, [13]C: Me_4Si; [19]F: CCl_3F; [199]Hg: Me_2Hg). Acetone-d_6 was used as an external lock (5 mm tube) in reaction control measurements while an original sample of the reaction mixture was measured in a 4 mm insert. Negative ESI-mass spectra in MeCN solutions were run on a Finnigan MAT 900 apparatus with a flow rate of 2 µl/min. EI mass spectra were recorded with a Finnigan MAT 95 spectrometer (20 eV). Intensities are referenced to the most intense peak of a group. Isotope patterns were calculated for comparison with the program ISOPRO [39]. Visible decomposition points were determined using the HWS Mainz 2000 apparatus. C, H and N analyses were carried out with a HEKAtech Euro EA 3000 apparatus. Details of crystal data and structure refinement parameters for $[PNP][Ag(C_5F_4N)_2]$ (1), $Hg(C_5F_4N)_2$ (2), $Ga(C_5F_4N)_3 \cdot EtCN \cdot H_2O$ (3), $In(C_5F_4N)_3 \cdot 2EtCN$ (4), and $Sn(C_5F_4N)_4$ (5) are summarised in Table 1.

4H-C_5F_4N was prepared according to [40] at 0 °C, [PNP]Cl according to [41]. AgF (Apollo) and all metals were used as received. EtCN was purchased from Acros Chemicals and used without further purification.

3.0.1. 4-Trimethylsilyl-2,3,5,6-tetrafluoropyridine, $Me_3SiC_5F_4N$

14.5 g C_5HF_4N (97 mmol) were dissolved in 80 mL Et_2O at −60 °C. 48.5 mL of a 2 M solution of n-BuLi (97 mmol) in n-pentane were dropped into the well-stirred solution. After stirring for 1 h, temperature was increased to −40 °C and 12.3 mL (97 mmol) of freshly distilled Me_3SiCl were dropped to the reaction mixture. After gentle warming to room temperature, LiCl was filtered off, and low boiling compounds were distilled at a bath temperature not exceeding 116 °C (Et_2O, n-pentane, C_5HF_4N) on a rotation evaporator. The remaining brown, oily residue was stored over Na_2SO_4 overnight, and finally the product was condensed in vacuo. 16.8 g $Me_3SiC_5F_4N$ (77% yield) were isolated as a colourless liquid.

^{19}F NMR (188.3 MHz, neat): $\delta = -94.2$ (m, 2F, F-2,6); −131.3 (m, 2F, F-3,5).

^{1}H NMR (200.1 MHz, neat): $\delta = 0.5$ (s, Me_3Si).

^{13}C NMR (50.3 MHz, neat): $\delta = 143.8$ (dm, $^1J_{F,C} \approx 251$ Hz, C-2,6); 142.5 (dm, $^1J_{F,C} \approx 247$ Hz, C-3,5); 132.2 (t, $^2J_{F,C} \approx 61$ Hz, C-4); −2.3 (q, $^1J_{C,H} \approx 121$ Hz, Me_3Si).

Analytical data matched with the literature values [42].

3.1. Crystal structure analyses

All compounds 1–5 [43] form colourless single crystals which were sealed in glass capillaries. Suitability was checked with the help of an IP-diffractometer (STOE IPDS II) [44,45]. The same device was used to collect the reflection data of the respective best specimen. The positions of the heavy atoms were extracted from these data using the direct methods provided by the program SHELXS-97 [46]. The light atoms were localised during the refinement (SHELXL-93) by difference Fourier syntheses [47]. Tilted angles were calculated with the program PARST-97 [48].

3.2. 4-Tetrafluoropyridylsilver propionitrile adduct, $AgC_5F_4N \cdot EtCN$

By analogy to [8], 0.25 g (2.0 mmol) AgF were suspended in 5 mL EtCN at ambient temperature. 0.46 g (2.1 mmol) $Me_3SiC_5F_4N$ were added and the mixture was stirred for 2 h. The colourless solution was taken off by a pipette and all volatile compounds were distilled off in vacuo at ambient temperature. Colourless, amorphous material was obtained in nearly quantitative yield which was sensitive to moisture and light.

^{19}F NMR (188.3 MHz, EtCN): $\delta = -98.9$ (m, 2F, F-2,6); −114.1 (m, 2F, F-3,5).

^{13}C NMR (50.3 MHz, CD_2Cl_2/CD_3CN): $\delta = 152.0$ (t, $^2J_{F,C} \approx 76$ Hz, C-4); 145.8 (dm, $^1J_{F,C} \approx 228$ Hz, C-2,6); 142.5 (dm, $^1J_{F,C} \approx 247$ Hz, C-3,5); 121.3 (broad, CH_3CH_2CN); 10.7 (tq, CH_3CH_2CN); 10.1 (qt, CH_3CH_2-CN).

Negative ESI-MS (MeCN): m/z (rel. int.): 924 $[Ag_3(C_5F_4N)_4]^-$ (1), 665 $[Ag_2(C_5F_4N)_3]^-$ (100), 407 $[Ag(C_5F_4N)_2]^-$ (76).

3.3. Bis(triphenylphosphoranyliden)ammonium bis (4-tetrafluoropyridyl)argentate, $[PNP][Ag(C_5F_4N)_2]$

To a solution of ca. 2.0 mmol AgC_5F_4N prepared as described above, 0.64 g (1.0 mmol) of [PNP]Cl dissolved in EtCN were added. Directly after combining both solutions, AgCl precipitated which was filtered off. The resulting solution was evaporated to dryness. After washing with n-pentane, colourless crystals of $[PNP][Ag(C_5F_4N)_2]$ were grown on storing a CH_2Cl_2/Et_2O mixture for several days at −20 °C. Colourless, crystalline $[PNP][Ag(C_5F_4N)_2]$ was obtained in 96% yield. ^{19}F and ^{13}C NMR and negative ESI spectra matched with those of $AgC_5F_4N \cdot EtCN$. Results of XRD measurements are described in Section 2.2.

Anal. Calc. for $C_{46}H_{30}F_8N_3AgP_2$: C, 58.36; H, 3.19; N, 4.44. Found: C, 57.64; H, 3.44; N, 3.55%.

3.4. Transmetallations with group 12 metals

3.4.1. Reactions with elemental zinc and cadmium

Transmetallations of AgC_5F_4N with zinc and cadmium were terminated after 16 h of heating to 75 °C in EtCN. After all AgC_5F_4N had been consumed, ^{19}F NMR spectra exclusively exhibited the signals of $Zn(C_5F_4N)_2$ ($\delta = -98.2$, −123.4) and $Cd(C_5F_4N)_2$ ($\delta = -97.6$, −119.2), respectively. With the knowledge that $Zn(R_f)_2$ and $Cd(R_f)_2$ form

1:2 complexes with donor molecules [14] together with the fact that $Zn(C_5F_4N)_2$ and $Cd(C_5F_4N)_2$ are known from the literature [49], no further efforts were made to obtain crystalline derivatives from the waxy raw materials.

3.4.2. Bis(4-tetrafluoropyridyl)mercury, $Hg(C_5F_4N)_2$

The reaction of AgC_5F_4N and a manifold excess of elemental mercury proceeded selectively at room temperature within a few minutes to give $Hg(C_5F_4N)_2$. Starting from 2.0 mmol AgF and 2.1 mmol $Me_3SiC_5F_4N$, 0.45 g $Hg(C_5F_4N)_2$ (45% yield) were isolated after distilling off all volatile compounds and subliming the residue in vacuo at ca. 150 °C. Colourless single crystals of $Hg(C_5F_4N)_2$ were obtained from CH_2Cl_2 or *n*-pentane solutions. The melting point (195–196 °C) agreed with the literature values of 193 °C [49] and 201–202 °C [50].

^{19}F NMR (188.3 MHz, CD_3CN): $\delta = -93.8$ (m, $^4J_{Hg,F} \approx 108$ Hz, 2F, F-2,6); -123.2 (m, 2F, $^3J_{Hg,F} \approx 371$ Hz, F-3,5).

^{13}C NMR (50.3 MHz, CD_3CN): $\delta = 153.3$ (t, $^2J_{F,C} \approx 46$ Hz, $^1J_{Hg,C} \approx 1734$ Hz, C-4); ≈ 145 (overlapping dm, C-2,6 and C-3,5).

^{199}Hg NMR (71.7 MHz, CD_3CN): $\delta = -1029$ (qiqi, $^3J_{Hg,F} \approx 370$ Hz, $^4J_{Hg,F} \approx 109$ Hz).

EI-MS (20 eV): m/z (rel. int.): 501 $[Hg(C_5F_4N)_2]^+$ (100), 351 $[Hg(C_5F_4N)]^+$ (25), 150 $[C_5F_4N]^+$ (50).

Anal. Calc. for $C_{10}F_8N_2Hg$: C, 31.68; N, 7.39. Found: C, 32.58; N, 7.28%.

3.5. Transmetallations with group 13 metals

3.5.1. Reactions with elemental gallium and indium

Reactions of AgC_5F_4N and elemental aluminium remained unsuccessful due to the passivation of the aluminium shot used. Reactions with elemental thallium proceeded with formation of a silver mirror but stopped on the thallium oxidation state of +I due to the too low oxidation potential of Ag^I. In reactions with excess of elemental gallium, signals of $Ga(C_5F_4N)_3$ ($\delta = -97.0, -127.1$) and the corresponding gallate, $[Ag \cdot nEtCN][Ga(C_5F_4N)_4]$ ($\delta = -95.4, -127.8$) were found in the ^{19}F NMR spectrum (integrative ratio = 2.4:1). Single crystals were grown from the raw material in *n*-pentane solutions over a period of two months at -21 °C in NMR tubes sealed with Parafilm®. XRD measurements proved the formation of the gallium species $Ga(C_5F_4N)_3 \cdot EtCN \cdot H_2O$ (Section 2.5).

EI-MS (20 eV): m/z (rel. int.): 519 $[Ga(C_5F_4N)_3]^+$ (100), 369 $[Ga(C_5F_4N)_2]^+$ (62), 243 (?) (26), 151 $[C_5HF_4N]^+$ (90).

NMR data cannot be provided due to very low solubility of the crystals in common organic solvents.

3.5.2. Tris(4-tetrafluoropyridyl)dipropionitrile indium, $In(C_5F_4N)_3 \cdot 2EtCN$

To a solution of AgC_5F_4N prepared from 4.0 mmol AgF and 4.2 mmol $Me_3SiC_5F_4N$ in EtCN elemental indium (shots, 1–3 mm) was added in large excess. The reaction mixture was stirred for 3 h at ambient temperature.

Complete conversion of the silver compound was controlled by ^{19}F NMR spectroscopic means. After a total reaction time of 3 h, all volatile components were distilled off in vacuo giving a metallic grey residue which was extracted with CH_2Cl_2 in a Soxhlet-apparatus. $In(C_5F_4N)_3 \cdot 2EtCN$ (m.p. 126–130 °C (loss of EtCN)) was obtained as a colourless solid in 35% yield (0.94 g). Crystals suitable for XRD measurements were grown from concentrated EtCN solutions at -28 °C (Section 2.6).

^{19}F NMR (188.3 MHz, $(CD_3)_2CO$); $\delta = -95.3$ (m, 2F, F-2,6); -122.3 (m, 2F, F-3,5).

^{1}H NMR (200.1 MHz, $(CD_3)_2CO$): $\delta = 2.45$ (q, $^3J_{HH} = 7.7$ Hz, 2H, CH_3CH_2CN); 1.24 (t, $^3J_{HH} = 7.7$ Hz, 3H, CH_3CH_2CN).

^{13}C NMR (50.3 MHz, $(CD_3)_2CO$): $\delta = 145.6$ (dm, $^1J_{F,C} \approx 247$ Hz, C-2,6); 143.6 (dm, $^1J_{F,C} \approx 247$ Hz, C-3,5); 121.6 (broad, CH_3CH_2CN and C-4); 10.8 (tq, CH_3CH_2CN); 10.7 (qt, CH_3CH_2CN).

EI-MS (20 eV): m/z (rel. int.): 565 $[In(C_5F_4N)_3]^+$ (26), 415 $[In(C_5F_4N)_2]^+$ (100), 151 $[C_5HF_4N]^+$ (17).

Anal. Calc. for $C_{21}H_{10}N_5F_{12}In$: C, 36.64; N, 9.46; H, 1.28. Found: C, 37.36; N, 10.37; H, 1.49%.

3.6. Tetrakis(4-tetrafluoropyridyl)tin, $Sn(C_5F_4N)_4$

To a solution of AgC_5F_4N prepared from 4.0 mmol AgF and 4.2 mmol $Me_3SiC_5F_4N$ in EtCN elemental tin was added in a manifold excess. The reaction mixture was stirred for 16 h at ambient temperature. After this period, signals of AgC_5F_4N were no longer detected in the ^{19}F NMR spectrum of the reaction mixture. All volatile components were distilled off in vacuo. The raw material was sublimed at ca. 230 °C/0.1 mbar for several hours giving a colourless material which was recrystallized from boiling EtCN/*n*-hexane in an open beaker. 0.15 g (20% yield) $Sn(C_5F_4N)_4$ were obtained as colourless needles with a melting point of 275 °C. The very low solubility in common organic solvents prevented from recording ^{13}C and ^{119}Sn NMR spectra.

^{19}F NMR (188.3 MHz, EtCN): $\delta = -91.4$ (m, 2F, F-2,6); -123.7 (m, 2F, F-3,5).

EI-MS (20 eV): m/z (rel. int.): 720 $[Sn(C_5F_4N)_4]^+$ (100), 570 $[Sn(C_5F_4N)_3]^+$ (42), 151 $[C_5HF_4N]^+$ (16).

Anal. Calc. for $C_{20}N_4F_{20}Sn$: C, 33.41; N, 7.79. Found: C, 33.59; N, 7.82%.

Acknowledgements

References

[1] (a) For example: M. Ferrer, M. Mounir, L. Rodríguez, O. Rossell, S. Coco, P. Gómez-Sal, A. Martín, J. Organomet. Chem. 690 (2005) 2200;

(b) D. Noveski, T. Braun, B. Neumann, A. Stammler, H.-G. Stammler, Dalton Trans. (2004) 4106;

(c) N.A. Jassim, R.N. Perutz, A.C. Whitwood, T. Braun, J. Izundu, B. Neumann, S. Rothfeld, H.-G. Stammler, Organometallics 23 (2004) 6140;

(d) B.V. Nguyen, D.J. Burton, J. Fluorine Chem. 67 (1994) 205;

(e) E.J. Soloski, W.E. Ward, C. Tamborski, J. Fluorine Chem. 2 (1973) 361;

(f) J. Cooke, M. Green, F.G.A. Stone, Inorg. Nucl. Chem. Lett. 3 (1967) 47;

(g) B.L. Booth, R.N. Haszeldine, J. Organomet. Chem. 6 (1966) 570.

[2] A.O. Miller, V.I. Krasnov, D. Peters, V.E. Platonov, R. Mietchen, Tetrahedron Lett. 41 (2000) 3817.

[3] (a) For example: R.G. Kultyshev, G.K.S. Prakash, G.A. Olah, J.W. Faller, J. Parr, Organometallics 23 (2004) 3184;

(b) V.V. Bardin, L.S. Pressman, G.G. Furin, J. Organomet. Chem. 448 (1993) 55.

[4] B. Hoge, C. Thösen, T. Herrmann, P. Panne, I. Pantenburg, J. Fluorine Chem. 125 (2004) 831.

[5] W.E. Tyrra, J. Fluorine Chem. 112 (2001) 149.

[6] W. Tyrra, Heteroatom. Chem. 13 (2002) 561.

[7] W. Tyrra, D. Naumann, J. Fluorine Chem. 125 (2004) 823.

[8] W. Tyrra, M.S. Wickleder, Z. Anorg. Allg. Chem. 628 (2002) 1841.

[9] D. Naumann, W. Wessel, J. Hahn, W. Tyrra, J. Organomet. Chem. 547 (1997) 79.

[10] S. Aboulkacem, W. Tyrra, I. Pantenburg, J. Chem. Crystallogr., in press.

[11] R.R. Burch, J.C. Calabrese, J. Am. Chem. Soc. 108 (1986) 5359.

[12] P.M. Jeffries, S.R. Wilson, G.S. Girolami, J. Organomet. Chem. 449 (1993) 203.

[13] R. Usón, A. Laguna, A. Usón, P.G. Jones, K. Meyer-Bäse, J. Chem. Soc., Dalton Trans. (1988) 341.

[14] (a) For Zn: H. Lange, D. Naumann, J. Fluorine Chem. 26 (1984) 435;

(b) D. Naumann, C. Schorn, W. Tyrra, Z. Anorg. Allg. Chem. 625 (1999) 827;

(c) For Cd: H. Lange, D. Naumann, J. Fluorine Chem. 26 (1984) 1;

(d) D. Naumann, K. Glinka, W. Tyrra, Z. Anorg. Allg. Chem. 594 (1991) 95.

[15] S. Aboulkacem, W. Tyrra, unpublished results.

[16] (a) F. Schulz, I. Pantenburg, D. Naumann, Z. Anorg. Allg. Chem. 629 (2003) 2312;

(b) D. Naumann, F. Schulz, I. Pantenburg, W. Tyrra, Z. Anorg. Allg. Chem. 630 (2004) 529.

[17] (a) G.B. Deacon, C.M. Forsyth, D.M.M. Freckmann, G. Meyer, D. Stellfeldt, Z. Anorg. Allg. Chem. 626 (2000) 540;

(b) D.L. Wilkinson, J. Riede, G. Müller, Z. Naturforsch. B 51 (1991) 285;

(c) D.S. Brown, A.G. Massey, D.A. Wickens, J. Organomet. Chem. 194 (1980) 131.

[18] D. Naumann, F. Schulz, Z. Anorg. Allg. Chem. 631 (2005) 122.

[19] G.B. Deacon, P.C. Junk, J. Chem. Crystallogr. 33 (2003) 605.

[20] K.-F. Tebbe, T. Gilles, F. Conrad, W. Tyrra, Acta Crystallogr., Sect. C 52 (1996) 1663.

[21] I.A. Guzei, S. Dagorne, R.F. Jordan, Acta Crystallogr., Sect. C 56 (2000) e134.

[22] A.H. Cowley, C.L.B. Macdonald, J.S. Silverman, J.D. Gorden, A. Voigt, Chem. Commun. (2001) 175.

[23] B.L. Kaafarani, H. Gu, A.A. Pinkerton, D.C. Neckers, J. Chem. Soc., Dalton Trans. (2002) 2318.

[24] M.-C. Chen, J.A.S. Roberts, T.J. Marks, Organometallics 23 (2004) 932.

[25] F. Conrad, Dissertation, Universität zu Köln, 1996.

[26] Cf. Ref [22], therein [5]; CCDC 137250.

[27] (a) C. Meyer, Dissertation, Universität Düsseldorf, 1994;

(b) F. Conrad, Z.-H. Choi, K. Ludovici, W. Tyrra, in: Proceedings of the 11th European Symposium on Fluorine Chemistry, Bled, Slovenia, 1995, Abstract 116.

[28] W. Tyrra, M.S. Wickleder, J. Organomet. Chem. 677 (2003) 28.

[29] H. Schumann, O. Just, Th.D. Seuß, F.H. Görlitz, R. Weimann, J. Organomet. Chem. 466 (1994) 5.

[30] Z.-H. Choi, W. Tyrra, A. Adam, Z. Anorg. Allg. Chem. 625 (1999) 1287.

[31] J. Emsley, The Elements, third ed., Clarendon Press, Oxford, 1998.

[32] A. Bondi, J. Phys. Chem. 68 (1964) 441;

S.C. Nyburg, C.H. Faerman, Acta Crystallogr., Sect. B 41 (1985) 274.

[33] R.D. Schluter, G. Krauter, W.S. Rees Jr., J. Cluster Sci. 8 (1997) 123, CA 126:324477; ROLREP.

[34] L.M. Engelhardt, L.-P. Leung, C.L. Raston, A.H. White, Aust. J. Chem. 35 (1982) 2383.

[35] I. Wharf, F. Bélanger-Gariépy, Acta Crystallogr., Sect. E 59 (2003) m661.

[36] A. Karipides, C. Forman, R.H.P. Thomas, A.T. Reed, Inorg. Chem. 13 (1974) 811.

[37] I. Ara, J. Forniés, M.A. García-Monforte, A. Martín, B. Menjón, Chem. Eur. J. 10 (2004) 4186.

[38] I. Wharf, A.-M. Lebuis, Acta Crystallogr., Sect. E 59 (2003) m794.

[39] M. Senko, ISOPRO 3.0, Shareware, Sunnyvale, CA.

[40] S.S. Laev, V.D. Shteingarts, Tetrahedron Lett. 38 (1997) 3765.

[41] J.K. Ruff, W.J. Schlientz, Inorg. Synth. 15 (1974) 84.

[42] R.E. Banks, R.N. Haszeldine, E. Philips, I.M. Young, J. Chem. Soc. C (1967) 2091.

[43] Crystallographic data for the structures have been deposited with the Cambridge Crystallographic Data Centre as supplementary publication nos. CCDC 272520 for **1**, CCDC 272522 for **2**, CCDC 274915 for **3**, CCDC 272521 for **4**, and CCDC 272519 for **5**. Copies of the data can be obtained, free of charge, on application to CCDC, 12 Union Road, Cambridge CB2 1EZ, UK (fax: +44 1223 336 033 or e-mail: deposit@ccdc.cam.ac.uk).

[44] X-RED 1.22, Stoe Data Reduction Program © 2001 Stoe & Cie GmbH Darmstadt.

[45] X-Shape 1.06, Crystal Optimisation for Numerical Absorption Correction © 1999 STOE & Cie GmbH Darmstadt.

[46] G.M. Sheldrick, SHELXS-97: Program for Structure Analysis, University of Göttingen, Göttingen, Germany, 1998.

[47] G.M. Sheldrick, SHELXL-93: Program for Crystal Structure Refinement, University of Göttingen, Göttingen, Germany, 1993.

[48] M. Nardelli, PARST-97, J. Appl. Crystallogr. 28 (1995) 659.

[49] P. Sartori, H. Adelt, J. Fluorine Chem. 3 (1973/74) 275.

[50] R.D. Chambers, F.G. Drakesmith, J. Hutchinson, W.K.R. Musgrave, Tetrahedron Lett. 18 (1967) 1705.